Asymptotical Computations for a Model of Flow in Saturated Porous Media

P. Amodio [a], C.J. Budd [b], O. Koch [c,*], G. Settanni [d], E. Weinmüller [c]

[a] *Dipartimento di Matematica, Università di Bari via E. Orabona 4, 70125 Bari, Italy*

[b] *Mathematical Sciences, University of Bath Bath BA2 7AY, United Kingdom*

[c] *Institute for Analysis and Scientific Computing (E101), Vienna University of Technology, Wiedner Hauptstrasse 8–10, A-1040 Wien, Austria*

[d] *Dipartimento di Matematica e Fisica 'E. De Giorgi', Università del Salento, via per Arnesano, 73047 Monteroni di Lecce, Lecce, Italy*

Abstract

We discuss an initial value problem for an implicit second order ordinary differential equation which arises in models of flow in saturated porous media such as concrete. Depending on the initial condition, the solution features a sharp interface with derivatives which become numerically unbounded. By using an integrator based on finite difference methods and equipped with adaptive step size selection, it is possible to compute the solution on highly irregular meshes. In this way it is possible to verify and predict asymptotical theory near the interface with remarkable accuracy.

Key words: Flow in concrete; Interface problem; Adaptive mesh selection; Asymptotic theory.
1991 MSC: 65L05; 65L12; 34E99.

* Corresponding author.
Email addresses: pierluigi.amodio@uniba.it (P. Amodio), mascjb@bath.ac.uk (C.J. Budd), othmar@othmar-koch.org (O. Koch), giuseppina.settanni@unisalento.it (G. Settanni), e.weinmueller@tuwien.ac.at (E. Weinmüller).

1 Introduction and Problem Statement

A model for the time dependent flow of water through a variably saturated porous medium with exponential diffusivity, such as soil, rock or concrete is given by

$$\frac{\partial u}{\partial t} = \frac{\partial}{\partial x}\left(D(u)\frac{\partial u}{\partial x}\right), \quad x \in [0,\infty), \quad t > 0, \tag{1}$$

$$u(0,t) = u_i, \quad u(\infty,t) = u_o, \quad u_o < u_i, \qquad u(x,0) = u_0(x), \tag{2}$$

where $u(x,t)$ is the *saturation* and is the fraction by volume of the pore space occupied by the liquid a distance x into the porous medium, and

$$D(u) = D_0 e^{\beta u}, \qquad \beta \text{ large.}$$

In this problem the bulk of the liquid resides in the interval $x \in [0, x^*(t)]$ where the moving interface $x^*(t)$ is called the *wetting front*, and $u \ll 1$ if $x > x^*$. The solution changes very rapidly close to the wetting front, making (1) a challenging problem both in analysis and in computation. The physical derivation of this equation is given in [8], [12], [15]. The numerical treatment of this problem was first discussed in [20]. A comprehensive overview of numerical methods for flow in porous media is given for instance in [11]. Similarity solutions of the problem have been studied extensively in earlier work and . [13] gives a comprehensive overview of analytical results for various types of nonlinear diffusion equations. In [13], the similarity solution for exponential diffusivity (3)–(5) below is derived. In [18], an iterative approach to solving this problem is developed. The paper [6] derives an asymptotic series expansion for the similarity solution under certain simplifying assumptions. Further asymptotic analysis of the similarity solution is developed in [16,17]. However, there has been a lack both of sharp asymptotic results and of convincing numerical calculations.

In the present paper we adopt a sophisticated numerical approach to investigate the asymptotical behavior of such self-similar solutions of the equation (1). These are stable attractors and take the form

$$u(x,t) = \psi(y), \quad y = x/t^{1/2}, \quad 0 < y < \infty.$$

If we set

$$\theta(y) = e^{\beta(\psi(y) - u_i)}$$

it then follows that $\theta(y)$ satisfies the ordinary differential equation boundary value problem

$$\theta(y)\theta_{yy}(y) = -y\theta_y(y), \quad y > 0, \tag{3}$$
$$\theta(0) = 1, \quad \theta(\infty) = \theta_\infty \equiv \mathrm{e}^{\beta(u_o - u_i)}. \tag{4}$$

It is convenient, for both the analysis and computation of this system to consider instead the initial value problem

$$\theta_y(0) = -\gamma < 0, \quad \theta(0) = 1. \tag{5}$$

and to determine the value of γ corresponding to θ_∞. The purpose of this paper is to make a numerical study of the solutions of (3)–(5) in the limit of large γ which corresponds to a problem with $\beta \gg 1$ with large diffusion when u is not small. The motivation for this investigation is to study a series of refined asymptotic estimates developed in [9] which significantly improve the earlier estimates. A second motivation is that the extreme nature of the problem and the existence of true asymptotical results gives an important test and validation of the numerical method described in this paper.

A plot of the solution $\theta(y)$ of (3)–(5) for $\gamma = 3$ is given in Figure 1. In this plot we can see that for smaller values of y the solution $\theta(y)$ decreases almost linearly, coming close to zero at the point $y \approx 1/\gamma$. As θ approaches zero it follows from (3)–(5) that θ_{yy} increases. Indeed, we can see from the figure that the solution has high positive curvature close to this point. For larger values of y the solution asymptotes to a constant value so that

$$\theta(y) \to \theta_\infty \quad \text{as} \quad y \to \infty.$$

Of interest are both θ_∞ and the point y^* (a rescaling of the wetting front x^*) at which θ_{yy} takes its maximum value, so that

$$\theta_{yyy}(y^*) = 0. \tag{6}$$

In analogy to the time-dependent problem we will refer to the latter as the *wetting front*. Indeed, if $y < y^*$ then $\theta = \mathcal{O}(1)$ and if $y > y^*$ then $\theta = \mathcal{O}(e^{-\gamma^2})$. An asymptotic study of this problem for *large* values of γ is given in [9], the results of which are summarised in Section 1. One purpose of this paper is to use an accurate high order numerical method to examine the asymptotic predictions of the latter paper and to accurately determine both the location of the wetting front and the value of θ_∞.

This problem poses a significant numerical challenge. Whilst the error terms in the asymptotic expansions (say of y^*) decay *polynomially* in γ as γ increases, it is shown in [9] that the curvature and final value are exponential in γ, that is

$$\theta_{yy}(y^*) \sim e^{\gamma^2} \quad \text{and} \quad \theta_\infty \sim e^{-\gamma^2}.$$

Hence, for even moderately large values of γ we see that the solution features a near-singularity in its higher derivatives, and moreover the solution is almost

identically equal to 0 for larger values of y. Indeed in the calculations reported in this paper we have values of $\theta_{yy} \sim 10^{138}$ and $\theta_\infty \sim 10^{-141}$. Conventional initial value solvers such as the Gear solvers in the MATLAB routine `ode15s` are unable to deal with the form of these singularities for values of γ at which the asymptotic results are expected to become sharp (for example values of $\gamma > 10$). For the larger values of γ required to study the asymptotic results a different numerical approach is required, and it is the difficulties described above that put this problem in the focus of the higher order methods that we will discuss in this paper. The numerical challenge is thus to find discretization schemes and adaptive mesh selection methods which are robust with respect to the dramatic variation in the stepsizes (up to 140 orders of magnitude in our computations reported below) which may be expected due to the predicted solution behavior as the curvature of θ rapidly increases. Earlier attempts in this direction have not been fully satisfactory, as the problem could only be solved for values of γ remote from the asymptotical regime [9].

Accordingly, in this paper we propose the construction of a variable step size numerical scheme directly for the second order problem (3)–(5) without resorting to a transformation to first order form. The idea of discretizing each derivative of the second order continuous problem by means of finite difference schemes has been largely considered in the past, in particular in the numerical solution of partial differential equations using schemes of low order (and with small stencils). In [4] and later in [1,3,5] it was proposed to apply high order finite difference schemes for the solution of boundary value problems for ordinary differential equations by considering different formulae with the same order in the initial and final points of the grid, following the idea inherited by *boundary value methods* [7]. One major advantage of this approach is associated with the fact that the vector of unknowns contains only the solution of the problem. This choice, on the one hand, reduces the computational cost of the algorithm with respect to the standard approaches which transform the second order equation into a first order one containing both the solution and its first derivative as unknowns. On the other hand, it simplifies the stepsize variation and allows the solution of fully implicit problems without any change in the approach. Moreover, in [14] it was demonstrated that a solution in the second order formulation may yield an advantage with respect to the conditioning of the linear systems of equations associated with the discretization scheme. Also, it is clear that in this approach, only the smoothness of the solution, but not of its derivative, affects the step-size selection process, see [10]. Finally, in the original formulation there is complete freedom in the choice of the schemes approximating each derivative which could not only depend on whether an initial or boundary value problem is solved, but also on the problem data and the discretization points. In [2] the same idea is applied to IVPs for ODEs. Two approaches are proposed to take care of the first derivative in the initial point: we can choose to approximate this initial condition by means of an appropriate formula or to define difference schemes which make use of

the analytical first derivative in the first point. As a general belief, the second approach seems to be preferable but, for the *flow in concrete* problem the first strategy is used, since the solution's derivative may be quite different from the solution itself (and hence affect the stepsize variation). The computations which enable to provide the mentioned results are only possible due to this highly flexible, adaptive finite difference method which is able to cope with extremely unsmooth step-size sequences. The numerical method is sufficiently good to not only confirm the asymptotical calculations in [9] but to also give a clear indication of the structure of further terms, which are currently beyond the reach of theoretical analysis.

The layout of the remainder of this paper is as follows. The numerical method is described in Section 2. Asymptotical solution properties are studied in Section 22. In Section 3.1, we briefly describe the asymptotic theory for (3)–(5) given in [9] and compare the results with our numerical simulations for values of $\gamma \leq 18$, for which $\theta_{yy}(y^*) \approx 10^{138}$ and $\theta_\infty \approx 10^{-141}$. In Section 3.2 a detailed analysis of the solution behaviour is given in the so-called *mid-range* of the independent variable in which $y \approx y^*$ and $\theta_{yy}(y)$ has very high values. We compare directly the asymptotical and numerical profiles. In Section 4 we show the form of the solution $\theta(y)$ and give plots of the solution and of its derivatives to illustrate the nature of the numerical difficulties and resulting errors described above. Finally in Section 5 we draw some conclusions from this work.

2 The Numerical Method

Here we describe the finite difference schemes underlying the computations presented in this manuscript. The coefficients in these multistep methods have been constructed via Taylor expansion such as to yield high-order approximations. The particular strength is the robustness with respect to large variations in the step-sizes which result from an adaptive procedure based on local error estimates computed by mesh halving. These have proven robust with respect to the unusually strong variations in the stepsizes encountered close to the points of high curvature experienced in this problem. The methods are applied to second-order initial value problems in their original formulation, and use different formulae for the appearing derivatives. The difference formulae are defined for equidistant grids and used on small subintervals of the time domain. Stepsize variation is performed after each subinterval as in the general block–BVM framework [7].

For the sake of clarity we consider the numerical solution of a general second

order initial value problem

$$\begin{cases} f(y, \theta, \theta_y, \theta_{yy}) = 0, \\ \theta(y_0) = \theta_0, \quad \theta_y(y_0) = \theta'_0. \end{cases} \tag{7}$$

We first specify an initial stepsize h_0 and a grid of equispaced points $Y = [y_0, y_1, \ldots, y_n]$, $y_i = y_0 + ih_0$. Denote the corresponding numerical approximation by

$$\Theta = [\theta_0,\ \theta_1,\ \ \ldots,\ \theta_n].$$

Following the idea in [2,4,5], we discretize separately the derivatives in (7) by means of suitable high order finite difference schemes

$$\theta^{(\nu)}(y_i) \simeq \theta_i^{(\nu)} = \frac{1}{h^\nu} \sum_{j=-s}^{r} \alpha_{s+j}^{(s,\nu)} \theta_{i+j}, \tag{8}$$

where $\nu = 1, 2$ represents the derivative index and $\alpha_{s+j}^{(s,\nu)}$ are the coefficients of the method which are fixed in order to reach the maximally possible order of accuracy. The integers s and r represent the number of left and right values required to approximate $\theta^{(\nu)}(y_i)$, and are strictly related to the order and the stability of the formula. For this problem we choose, when possible, $r = s$ obtaining formulae (called ECDF in [5]) of even order $p = 2s$ for both the first and the second derivative. For example, we have for

Order 4

$$h^2\ \theta_{yy}(y_i) \approx -\tfrac{1}{12}\theta_{i-2} + \tfrac{4}{3}\theta_{i-1} - \tfrac{5}{2}\theta_i + \tfrac{4}{3}\theta_{i+1} - \tfrac{1}{12}\theta_{i+2},$$

$$h\ \theta_y(y_i) \approx \tfrac{1}{12}\theta_{i-2} - \tfrac{2}{3}\theta_{i-1} + \tfrac{2}{3}\theta_{i+1} - \tfrac{1}{12}\theta_{i+2},$$

Order 6

$$h^2\ \theta_{yy}(y_i) \approx \tfrac{1}{90}\theta_{i-3} - \tfrac{3}{20}\theta_{i-2} + \tfrac{3}{2}\theta_{i-1} - \tfrac{49}{18}\theta_i + \tfrac{3}{2}\theta_{i+1} - \tfrac{3}{20}\theta_{i+2} + \tfrac{1}{90}\theta_{i+3},$$

$$h\ \theta_y(y_i) \approx -\tfrac{1}{60}\theta_{i-3} + \tfrac{3}{20}\theta_{i-2} - \tfrac{3}{4}\theta_{i-1} + \tfrac{3}{4}\theta_{i+1} - \tfrac{3}{20}\theta_{i+2} + \tfrac{1}{60}\theta_{i+3}.$$

We observe that the coefficients are symmetric and skew-symmetric for the second and first derivatives, respectively. We have successfully used these schemes up to the order 10.

We compute the unknowns in Θ by solving the nonlinear system

$$f(y_i, \theta_i, \theta_i^{(1)}, \theta_i^{(2)}) = 0, \qquad i = 1, \ldots, n-1, \tag{9}$$

together with the initial conditions. Since the above symmetric formulae of order $p > 2$ cannot be used to approximate $\theta^{(\nu)}(y_i)$, $i = 1, \ldots, p/2 - 1$ and

$i = n - p/2 + 1, \ldots, n - 1$, schemes in (8) with different stencils (but the same order) must be provided at the beginning and the end of the grid. We call them initial and final formulae (see [7]). Examples of the initial schemes are

Order 4

$$h^2\ \theta_{yy}(y_1) \approx \frac{5}{6}\theta_0 - \frac{5}{4}\theta_1 - \frac{1}{3}\theta_2 + \frac{7}{6}\theta_3 - \frac{1}{2}\theta_4 + \frac{1}{12}\theta_5,$$
$$h\ \theta_y(y_1) \approx -\frac{1}{4}\theta_0 - \frac{5}{6}\theta_1 + \frac{3}{2}\theta_2 - \frac{1}{2}\theta_3 + \frac{1}{12}\theta_4.$$

Order 6

$$h^2\ \theta_{yy}(y_1) \approx \frac{7}{10}\theta_0 - \frac{7}{18}\theta_1 - \frac{27}{10}\theta_2 + \frac{19}{4}\theta_3 - \frac{67}{18}\theta_4 + \frac{9}{5}\theta_5 - \frac{1}{2}\theta_6 + \frac{11}{180}\theta_7,$$
$$h^2\ \theta_{yy}(y_2) \approx -\frac{11}{180}\theta_0 + \frac{107}{90}\theta_1 - \frac{21}{10}\theta_2 + \frac{13}{18}\theta_3 + \frac{17}{36}\theta_4 - \frac{3}{10}\theta_5 + \frac{4}{45}\theta_6 - \frac{1}{90}\theta_7,$$
$$h\ \theta_y(y_1) \approx -\frac{1}{6}\theta_0 - \frac{77}{60}\theta_1 + \frac{5}{2}\theta_2 - \frac{5}{3}\theta_3 + \frac{5}{6}\theta_4 - \frac{1}{4}\theta_5 + \frac{1}{30}\theta_6,$$
$$h\ \theta_y(y_2) \approx \frac{1}{30}\theta_0 - \frac{2}{5}\theta_1 - \frac{7}{12}\theta_2 + \frac{4}{3}\theta_3 - \frac{1}{2}\theta_4 + \frac{2}{15}\theta_5 - \frac{1}{60}\theta_6.$$

The final schemes used to approximate $\theta^{(\nu)}(y_n)$ and, for the order 6, $\theta^{(\nu)}(y_{n-1})$, are not reported. Anyway, the coefficients of these methods correspond to the initial ones given above, but in reversed order and with the opposite sign in case of the first derivative. Note that for the second derivative, the order of the initial methods is $p = r + s - 1$ (we need one additional value to obtain the required order).

The number of grid points $n \geq p$ computed by solving (9) is linked to stability and computational cost. Larger n means better stability properties but higher computational cost [2,7]. For this problem we have fixed $n = p + 4$. The structure of the coefficient matrix associated with the second derivative for $p = 10$ is shown in Figure 2. In this example, the main scheme is applied five times and combined with four initial and final schemes. The size of the resulting matrix is $(n - 1) \times (n + 1)$, but the first column can be neglected because the starting value θ_0 is known. To complete the discretization, $\theta_y(0)$ is approximated by a suitable starting scheme obtained by choosing $s = 0$ in

(8). Examples of these latter formulae are:

Order 4:

$$h\theta_y(y_0) \approx -\tfrac{25}{12}\theta_0 + 4\theta_1 - 3\theta_2 + \tfrac{4}{3}\theta_3 - \tfrac{1}{4}\theta_4 = h\theta'_0,$$

Order 6:

$$h\theta_y(y_0) \approx -\tfrac{49}{20}\theta_0 + 6\theta_1 - \tfrac{15}{2}\theta_2 + \tfrac{20}{3}\theta_3 - \tfrac{15}{4}\theta_4 + \tfrac{6}{5}\theta_5 - \tfrac{1}{6}\theta_6 = h\theta'_0.$$

Once the solution in $y_i = y_0 + ih_0$, $i = 1, \ldots, n$, has been approximated, the stepsize is changed according to an estimate of the local relative error based on the mesh halving strategy and the algorithm is iterated on a subsequent subinterval. The code uses a classical time stepping strategy [19] with safety factor 0.7

$$h_{\text{new}} = \left(\frac{0.7\,tol}{\text{error}}\right)^{\frac{1}{(p+1)}} h_{\text{old}}.$$

In order to obtain the numerical approximations, for all the even orders from 4 to 10 we have used initial stepsize $h_0 = 1e-3$ and relative error tolerance $tol = 1e-12$ for both the solution and the Newton iteration. Moreover, we stress that the numerical solution is reliable having the computed stepsize the same order of magnitude of the solution and of its derivative.

Since however the second last values θ_{n-1} and θ'_{n-1} are better approximated than θ_n and θ'_n, we discard the last value in Θ, use formula (8) with $i = n-1$, $r = 1$ to compute θ'_{n-1}, and continue the algorithm with the initial conditions $[\theta_{n-1},\ \theta'_{n-1}]$.

3 Asymptotic Solution Properties

3.1 Asymptotics for Large γ

In this section we outline the main asymptotic predictions for the solutions of (3)–(5) which are presented in [9] and will show how these are supported by the numerical calculations. In [9] a matched asymptotic expansion method is used to find an asymptotic form of both the wetting front y^* defined in (6) as the point of maximal curvature and the final value of $\log(\theta_\infty)$, expressing both as formal asymptotic series expanded in powers of $1/\gamma$ with $\gamma \gg 1$. The asymptotic series are found by matching descriptions of the solution in an *inner range* with $y < y^* \approx 1/\gamma$, a *mid-range* with $y \approx y^*$ and an outer range

with $y \gg y^*$. It is in the mid-range where the most delicate behaviour occurs, with exponentially large (in γ) values for θ_{yy} making the asymptotic theory challenging in this case. We will describe the precise form of the solution in the mid-range in Section 3.2.

In [9] it is proposed that as $\gamma \to \infty$ the value of $\theta(1/\gamma)$ is given asymptotically by the expression

$$\theta\left(\frac{1}{\gamma}\right) = \frac{1}{2\gamma^2} - \frac{\log(\gamma)}{\gamma^4} + \frac{b}{\gamma^4}, \tag{10}$$

where

$$b = b^* + \mathcal{O}\left(\frac{1}{\gamma^2}\right) \quad \text{with} \quad b^* = \frac{11}{12} - \frac{1}{2}\log(2) \approx 0.57009307.... \tag{11}$$

Similarly, the final value θ_∞ satisfies the asymptotic relation

$$\log(\theta_\infty) = -\gamma^2 - \frac{1}{2} + \frac{\alpha}{\gamma^2}, \tag{12}$$

where it is conjectured that α takes the form

$$\alpha = \alpha^* + \mathcal{O}\left(\frac{1}{\gamma^2}\right), \tag{13}$$

with α^* an unknown constant. Furthermore, the location of the wetting front y^* is given asymptotically by the expression

$$y^* = \frac{1}{\gamma} + \frac{1}{2\gamma^3} + \frac{\beta}{\gamma^5}, \tag{14}$$

where

$$\beta = \beta^* + \mathcal{O}\left(\frac{1}{\gamma^2}\right), \quad \text{with} \quad \beta^* = \frac{11}{12}. \tag{15}$$

At the wetting front we have

$$\theta(y^*) \approx e\theta_\infty \quad \text{and} \quad \theta_{yy}(y^*) \approx \frac{e^{\gamma^2 - 1/2}}{\gamma^2} =: \hat{\theta}_{yy}. \tag{16}$$

Using the finite difference schemes described in the previous section, we study these asymptotic results by solving the initial value problem (3)–(5) for $\gamma = 2, 3, \ldots 18$. For $\gamma > 18$ the solution for large y where $\theta \approx \theta_\infty = 10^{-141} \sim e^{-\gamma^2}$ is too small to be computed accurately and for $\gamma > 26$ it is smaller than the smallest positive double precision machine number. Note that although $\gamma = 18$ poses a serious challenge for the numerical method, the predicted asymptotic error of order $1/\gamma^2$ is not unreasonably small. We considered methods of orders $p = 4,\ 6,\ 8$, and 10 to understand how the order of the numerical method

influences the accuracy of the approximate solutions. For the purpose of illustration, we will generally give the results for $p = 4$ and $p = 8$. As a general remark, we observe that the discretization errors are larger than the round-off errors of the floating point operations. Moreover, we propagate the solution using variable stepsizes, and for a fixed tolerance, methods of higher order allow for larger stepsizes but they do not necessarily achieve better precision. This is most probably due to the fact that higher derivatives of the solution θ are extremely unsmooth. The solution has been computed on finite intervals $[0, y_\infty]$, with the interval endpoint $y_\infty = 10, 20, 30, 40, 50$, to see how strongly the value of $\theta(y_\infty)$ depends on the length of the interval of integration. It turns out that, especially for large values of γ, the influence of the interval length is negligible. Therefore, from now on, we use the interval $[0, 10]$ and $\theta_\infty \approx \theta(10)$ for all calculations.

In Table 1 we present the results of the numerical computations of the various terms in the expressions above. All data are given for computations with $\gamma = 10$ and $\gamma = 18$, respectively. Since the reference values are asymptotically correct for large values of γ, we expect to observe higher accuracy for larger γ. In rows 1 and 2 of Table 1, we specify the values of θ_∞ and y^*, where y^* is defined to be the point where the numerically computed value of θ_{yy} takes its maximal value in the interval $[0, y_\infty] = [0, 10]$. In row 3 we first report the relative error in approximating $-\log(\theta_\infty)$ by $\gamma^2 + \frac{1}{2}$ and then in row 4 we compute an approximation for α as defined in (12). The values in row 3 confirm that the value of θ_∞ has been computed accurately (the relative error is always smaller than γ^{-4}) and the computed value for α in expression (12) is $\alpha \approx -0.08$.

Motivated by the relation (14) we define

$$s^* = \gamma^3 y^* - \gamma^2 = \frac{1}{2} + \mathcal{O}\left(\frac{1}{\gamma^2}\right). \tag{17}$$

In row 5 of Table 1 we specify the relative error $|s^* - 0.5|/0.5$ and in row 6 we use (14) to approximate the value of β. Again the relative error is smaller than γ^{-2} while the value of β is close to 0.95.

Rows 7 and 8 contain the numerical approximations of $\theta(y^*)$ and $\theta_{yy}(y^*)$, showing the very rapid increase in the value of the latter with γ. In rows 9 and 10 we specify the relative errors

$$\frac{|\theta(y^*) - e\theta_\infty|}{e\theta_\infty}, \qquad \text{and} \qquad \frac{\left|\theta_{yy}(y^*) - \hat{\theta}_{yy}\right|}{\hat{\theta}_{yy}}, \tag{18}$$

where $\theta(y^*)$ and $\theta_{yy}(y^*)$ denote our numerically obtained values. Finally, rows 11 and 12 contain the numerical value of b as given in (10) and the relative error. In all of these expressions the relative error decreases as γ increases,

demonstrating that to leading order both the numerical and asymptotic calculations are correct.

Given the relatively modest values of γ used in the computations, and the corresponding large asymptotic errors, it is necessary to post-process the numerical results to determine the finer structure of the solution and to verify the accuracy of the methods used. This post-processing allows us to make some further conjectures about the asymptotic solution. Taking the asymptotic expressions for α, β and b in expressions (10), (12), and (14) in the precise form

$$\alpha = \alpha^* + \frac{A}{\gamma^2}, \tag{19}$$

$$\beta = \beta^* + \frac{B}{\gamma^2}, \tag{20}$$

$$b = b^* + \frac{C}{\gamma^2}, \tag{21}$$

we substitute the results from Table 1 for $\gamma = 10$ and $\gamma = 18$ to find the corresponding values of $\alpha^*, \beta^*, b^*, A, B, C$. This calculation gives

$$\begin{array}{llll} \alpha^* \approx -0.0834 \approx -1.0004/12, & \text{with} & A \approx -0.089, \\ \beta^* \approx 0.9163 \approx 10.9954/12, & \text{with} & B \approx 2.96, \\ b^* \approx 0.5620 & \text{with} & C \approx 4.81. \end{array}$$

These results are close to the asymptotical results given in (15), (11) for which $\beta^* = 11/12 \approx 0.9166666$, and $b^* \approx 0.57009$, while the result for α^* strongly implies the new result that

$$\alpha^* = -\frac{1}{12}. \tag{22}$$

We conclude from this numerical calculation that there is strong evidence for the correctness of the asymptotic expressions in [9] and that the *wetting front* y^* is located at the point

$$y^* \approx \frac{1}{\gamma} + \frac{1}{2\gamma^3} + \frac{11}{12\gamma^5} + \frac{2.96}{\gamma^7}.$$

Moreover,

$$\log(\theta_\infty) \approx -\gamma^2 - \frac{1}{2} - \frac{1}{12\gamma^2} - \frac{0.089}{\gamma^4}.$$

Table 1
Asymptotic results: Part 1.

$\gamma = 10$		
Order	4	8
θ_∞	2.254440321030590e−44	2.254439903035485e−44
y^*	1.005094588206025e−01	1.005094588173695e−01
$\frac{\lvert\log(\theta_\infty)+\gamma^2+0.5\rvert}{\gamma^2+0.5}$	8.381534862525284e−06	8.383379735339227e−06
α	−8.423442536837911e−02	−8.425296634015922e−02
$\lvert s^*-0.5\rvert/0.5$	1.891764120503581e−02	1.891763473901165e−02
β	9.458820602506902e−01	9.458817369495821e−01
$\theta(y^*)$	6.126853837541197e−44	6.179228381160976e−44
$\theta_{yy}(y^*)$	1.648468426869335e+41	1.648412414631253e+41
$\frac{\lvert\theta(y^*)-e\theta_\infty\rvert}{e\theta_\infty}$	2.203452148159067e−04	8.326316736789704e−03
$\lvert\theta_{yy}(y^*)-\hat{\theta}_{yy}\rvert/\hat{\theta}_{yy}$	1.106641417450169e−02	1.103205980544998e−02
b	5.138760976981811e−01	5.138757975462900e−01
$\lvert b-\hat{b}\rvert/\hat{b}$	9.861017615723677e−02	9.861070265352932e−02

$\gamma = 18$		
Order	4	8
θ_∞	1.178498689884995e−141	1.178497239286140e−141
y^*	5.564177918914028e−02	5.564177918834908e−02
$\frac{\lvert\log(\theta_\infty)+\gamma^2+0.5\rvert}{\gamma^2+0.5}$	7.913110850624213e−07	7.951042681243711e−07
α	−8.319686486129285e−02	−8.359567254206013e−02
$\lvert s^*-0.5\rvert/0.5$	5.712462132123619e−03	5.712452903708254e−03
β	9.254188654173835e−01	9.254173704034648e−01
$\theta(y^*)$	3.198906899145607e−141	3.211721064871286e−141
$\theta_{yy}(y^*)$	9.664468728333972e+137	9.664458760222388e+137
$\frac{\lvert\theta(y^*)-e\theta_\infty\rvert}{e\theta_\infty}$	1.431149209001307e−03	2.570147096053791e−03
$\lvert\theta_{yy}(y^*)-\hat{\theta}_{yy}\rvert/\hat{\theta}_{yy}$	3.363040886020695e−03	3.362005998844594e−03
b	5.471501619326116e−01	5.471487116780027e−01
$\lvert b-\hat{b}\rvert/\hat{b}$	4.024415556753806e−02	4.024669945847258e−02

Next, we consider the asymptotical solution properties in the regime where y lies in the mid-range close to $y^* \approx 1/\gamma$. In this very delicate region where the solution changes rapidly, we compare the asymptotic form of the function with the numerical profiles. It is convenient to rescale both the dependent and independent variables in this region according to (17), such that

$$y = \frac{1}{\gamma} + \frac{s}{\gamma^3} \quad \text{and} \quad v(s) = \gamma^4 \theta(y),$$

with $|s|$ varying between 1 and γ^2.

We first discuss the case of negative s.

Case 1: Let $-\gamma^2 \ll s \ll -1$. In [9] an asymptotic series for the function $v(s)$ is developed in the form

$$v(s) = \gamma^2 v_0(s) + v_1(s) + O\left(\frac{1}{\gamma^2}\right). \tag{23}$$

A careful application of the method of matched asymptotic expansions then implies that

$$v_0(s) = \frac{1}{2} - s \tag{24}$$

and

$$v_1(s) = 2\log(\gamma)s - \log(\gamma) + b - \left(s - \frac{1}{2}\right)\log\left(\frac{1}{2} - s\right) + \frac{\log(2)}{2}, \tag{25}$$

where $b = \dfrac{11}{12} - \dfrac{1}{2}\log(2)$.

In Figures 3 and 4, we plot the values of $v_1(s)$ and their numerical approximations together with the relative errors (logarithmic scale), respectively. Computations were realized with the method of order 8. We can see the desired behaviour in the asymptotical regime $-\gamma^2 \ll s < 0$. Note furthermore that as expected the approximation improves as γ increases.

We next consider the mid-range with positive values of s. It is in this range that we see the rapid transition from polynomial to exponential decay.

Case 2: Let $1 \ll s \ll \gamma^2$. The asymptotic form of $v(s)$ is given by [9],

$$v(s) = v_\infty \left(1 + e^{-\gamma_e} e^{-(s-s^*)/v_\infty}\right), \tag{26}$$

where $s^* = \frac{1}{2} + O(1/\gamma^2)$ and $\gamma_e \approx 0.577215665$ is the Euler–Mascheroni constant. For a large value of γ the value of v_∞ is very small, and therefore, $v(s)$ in (26) is constant and coincides with $v_\infty \equiv \theta_\infty/\gamma^4$.

Figures 5 and 6 show the graphs of $v(s)$ and their absolute errors obtained based on (26), computed by the method of order 8 for $\gamma = 10$ and $\gamma = 18$, respectively. Note that in spite of the small solution values, the numerical results are still meaningful with an accuracy of about five digits. However, the very small value of the solution makes all comparisons difficult.

4 Accuracy of the Numerical Method

Finally, we demonstrate the numerical challenges and the resulting numerical errors encountered in the course of the computations which led to the results on the asymptotical solution behavior discussed in the previous sections. For larger values of γ, the solution features an interface with very large values of the second derivative. This can only be resolved with an adaptive step selection procedure which allows for extreme step-size variations without jeopardizing the stability of the computations.

In Fig. 7, we show the graphs in a logarithmic scale of the numerical solution and its first and second derivatives for the value $\gamma = 18$ computed by the numerical method of order 8. The rapid change in θ and its derivatives close to the wetting front is very clear from these figures. It was found that the approximation of the first and the second derivative becomes unreliable in the area where the solution becomes constant. In fact, since derivatives are computed by means of linear combinations of the solution values (using finite difference formulae (8)), it is really unlikely that they can be lower (in absolute value) than θ_∞EPS, where EPS is the machine precision, and in this case must be treated as 0.

Secondly, in Fig. 8 we plot the variation of the stepsizes for the methods of orders 4, 6, 8, and 10. The used tolerance is 1e−12 and the initial step size is 1e−3. We note that the orders 6 and 8 require the smallest number of meshpoints, since the size of each block is $p + 4$.[1] We observe the very small stepsizes used in these methods close to the point of high curvature. Note that the same minimal stepsize was defined for all orders, and this stepsize is reached with fewer but larger steps if the order of the method is higher.

[1] Clearly, the number of meshpoints is equal to $p + 4$ times the number of blocks (see Section 2).

5 Conclusions

We have discussed the numerical solution of a second–order ODE problem which arises as a model of flow through porous media. The solution of this problem features an interface with very large values of the higher derivatives. An adaptive finite difference method is employed to approximate the solution numerically and verify predictions derived by asymptotic theory.

The numerical investigation is successful. The solution algorithm can cope with a large variation in the stepsizes and thus can serve to accurately approximate the location of the interface and asymptotic characteristics of the solution.

In particular for the case where the interface is very sharp (blow-up of the second derivative), the simulations give very stable results which closely match the theoretical results, both in confirming certain of the asymptotic predictions for the location of the interface and the asymptotic value at infinity derived in [9] and also in giving strong evidence for further asymptotic results which are beyond the existing theory. This lends validity to both the numerical method and the asymptotic calculation.

Thus the asymptotic results and the numerical procedures are both verified, parameters not given by the a priori analysis are determined and new predictions about the solution structure are indicated.

Acknowledgment

We thank EU FP7 Marie Curie ITN FIRST for partly supporting this work. Moreover we would like to thank the referee for helpful and detailed comments on the presentation of the material in this manuscript, which have been a great help in improving the paper.

References

[1] P. Amodio and G. Settanni. Variable step/order generalized upwind methods for the numerical solution of second order singular perturbation problems. *JNAIAM J. Numer. Anal. Indust. Appl. Math.*, 4:65–76, 2009.

[2] P. Amodio and G. Settanni. High order finite difference schemes for the solution of second order initial value problems. *JNAIAM J. Numer. Anal. Indust. Appl. Math.*, 5:3–16, 2010.

[3] P. Amodio and G. Settanni, A finite differences MATLAB code for the numerical solution of second order singular perturbation problems. *J. Comput. Appl. Math.* 236:3869–3879, 2012.

[4] P. Amodio and I. Sgura. High-order finite difference schemes for the solution of second-order BVPs. *J. Comput. Appl. Math.*, 176:59–76, 2005.

[5] P. Amodio and I. Sgura. High order generalized upwind schemes and numerical solution of singular perturbation problems. *BIT*, 47:241–257, 2007.

[6] D.K. Babu. Infiltration analysis and perturbation methods. 1. Absorption with exponential diffusivity. *Water Resour. Res.*, 12:89–93, 1976.

[7] L. Brugnano and D. Trigiante. *Solving Differential Problems by Multistep Initial and Boundary Value Methods.* Gordon and Breach Science Publishers, Amsterdam, 1998.

[8] W. Brutsaert. Universal constants for scaling the exponential soil water diffusivity. *Water Resour. Res.*, 15(2):481–483, 1979.

[9] C.J. Budd and J. Stockie. Asymptotic behaviour of wetting fronts in porous media with exponential moisture diffusivity. Submitted, 2013.

[10] J. Cash, G. Kitzhofer, O. Koch, G. Moore, and E.B. Weinmüller. Numerical solution of singular two-point BVPs. *JNAIAM J. Numer. Anal. Indust. Appl. Math.*, 4:129–149, 2009.

[11] Z. Chen, G. Huan, and Y. Ma. *Computational Methods for Multiphase Flows in Porous Media.* SIAM, Philadelphia, PA, 2006.

[12] B. E. Clothier and I. White. Measurement of sorptivity and soil water diffusivity in the field. *Soil Sci. Soc. Amer. J.*, 45:241–245, 1981.

[13] J. Crank. *The Mathematics of Diffusion.* Oxford University Press, Oxford, U.K., 1975.

[14] G. Kitzhofer, O. Koch, P. Lima, and E.B. Weinmüller. Efficient numerical solution of the density profile equation in hydrodynamics. *J. Sci. Comput.*, 32:411–424, 2007.

[15] C. Leech, D. Lockington, and P. Dux. Unsaturated diffusivity functions for concrete derived from NMR images. *Mater. Constr.*, 34:413–418, 2003.

[16] J.-Y. Parlange. A note on a three-parameter soil–water diffusivity function — Application to the horizontal infiltration of water. *Soil Sci. Soc. Amer. J.*, 37:318–319, 1973.

[17] M.B. Parlange, S.N. Prasad, J.-Y. Parlange, and M.J.M. Römkens. Extension of the Heaslet–Alksne technique to arbitrary soil water diffusivities. *Water Resour. Res.*, 28:2793–2797, 1992.

[18] J.D. Parslow, D. Lockington, and J.-Y. Parlange. A new perturbation expansion for horizontal infiltration and sorptivity estimates. *Transp. Porous Media*, 3:133–144, 1988.

[19] W.H. Press, B.P. Flannery, S.A. Teukolsky, and W.T. Vetterling. *Numerical Recipes in C — The Art of Scientific Computing*. Cambridge University Press, Cambridge, U.K., 1988.

[20] M. Rose. Numerical methods for flows through porous media I. *Math. Comp.*, 40(162):435–467, 1983.

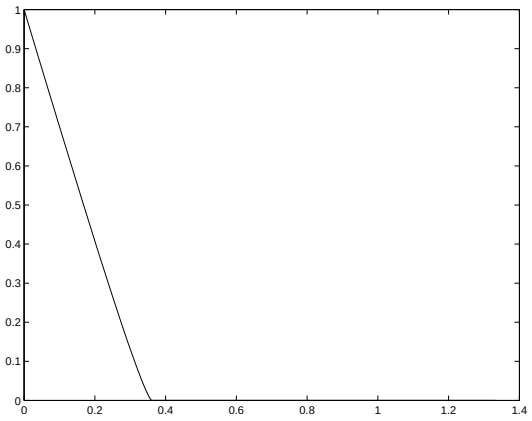

Fig. 1. The solution for $\gamma = 3$. In this figure we can see the initial linear decrease of the solution towards zero, the point of high curvature for $y = y^* \approx 1/3$ and the very small value assumed for $y > y^*$.

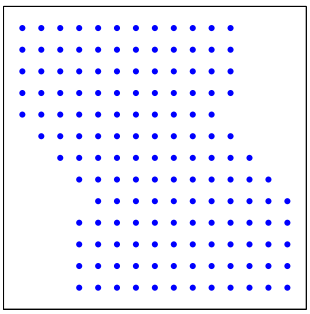

Fig. 2. Structure of the coefficient matrix approximating the second derivative, $p = 10$ and $n = p + 4$.

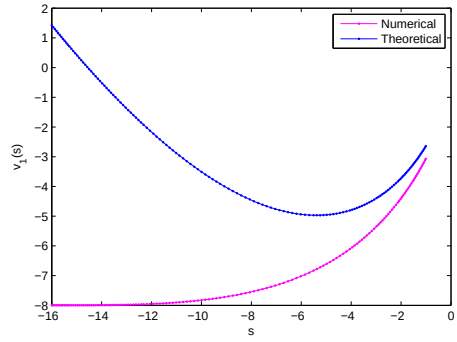

(a) $\gamma = 4$.

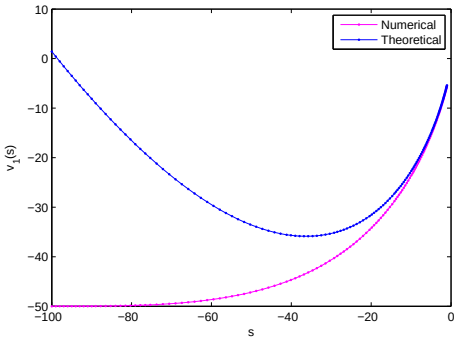

(b) $\gamma = 6$.

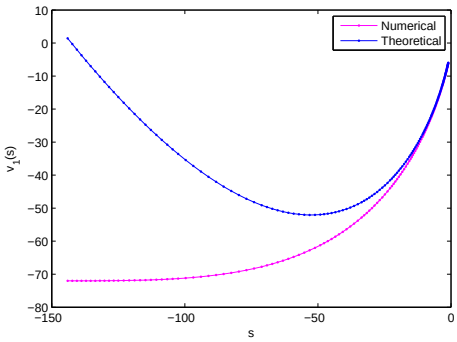

(c) $\gamma = 12$.

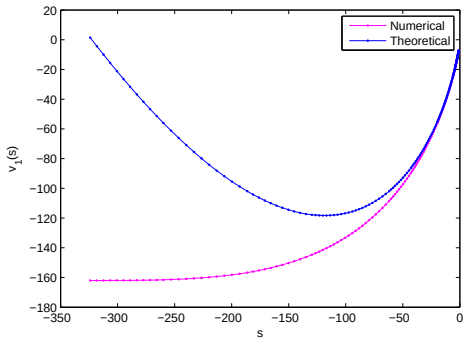

(d) $\gamma = 18$.

Fig. 3. Analytical values and numerical approximation for v_1, order 8.

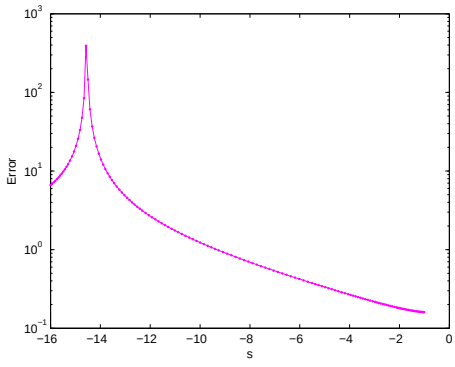

(a) $\gamma = 4$.

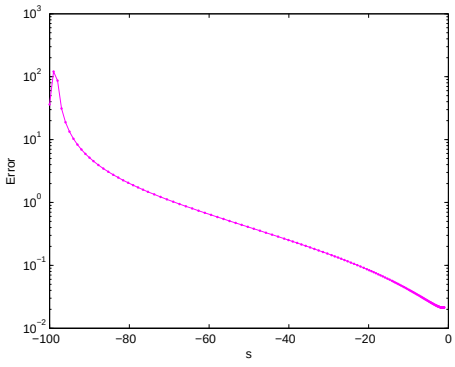

(b) $\gamma = 10$.

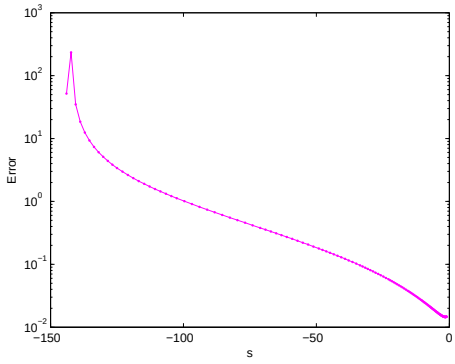

(c) $\gamma = 12$.

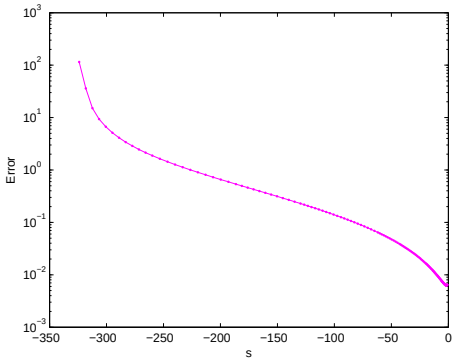

(d) $\gamma = 18$.

Fig. 4. Relative error of v_1, order 8.

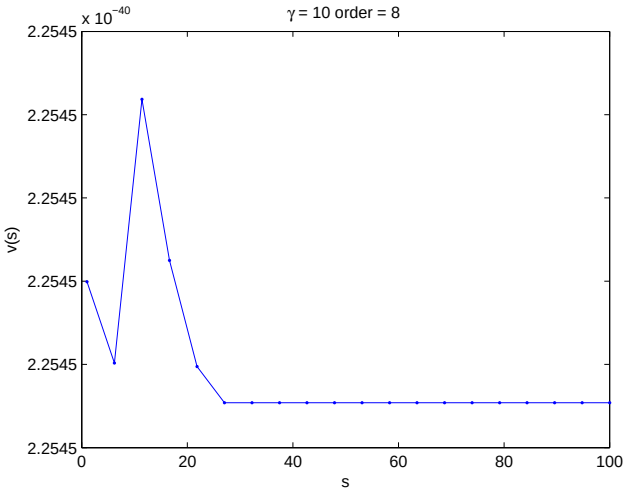

(a) $v(s)$, $\max_s |v(s)| = 2.254510924061732e - 040$

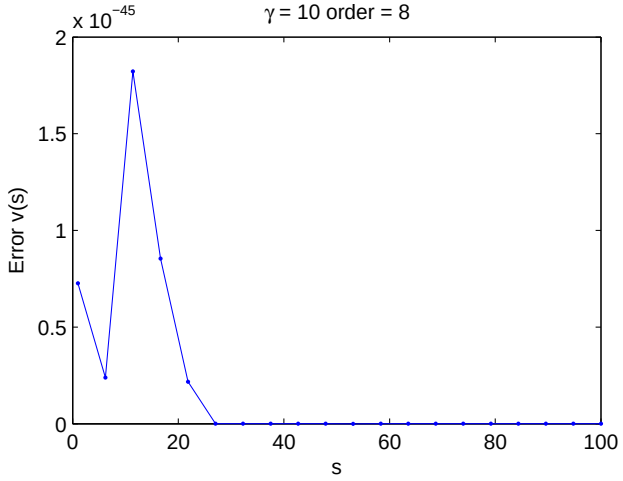

(b) Absolute error of $v(s)$

Fig. 5. $\gamma = 10$, order 8

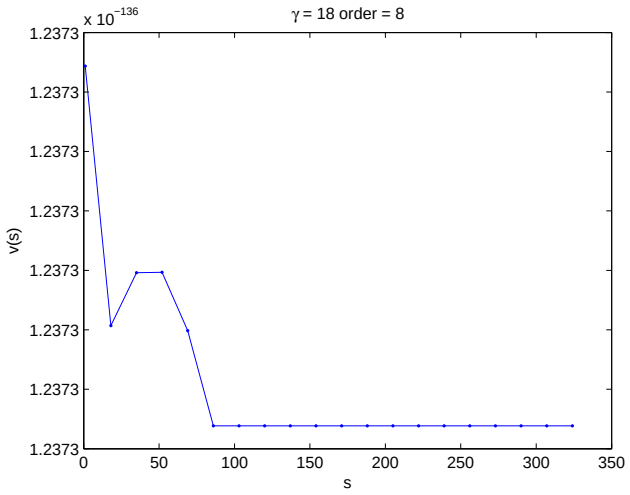

(a) $v(s)$, $\max_s |v(s)| = 1.237327181687361e - 136$

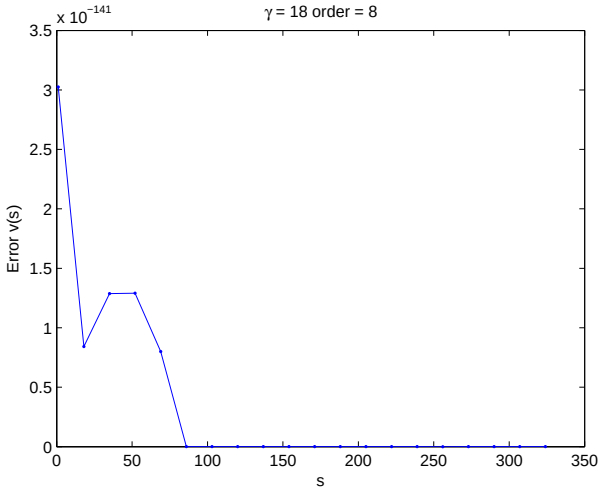

(b) Absolute error of $v(s)$

Fig. 6. $\gamma = 18$, order 8

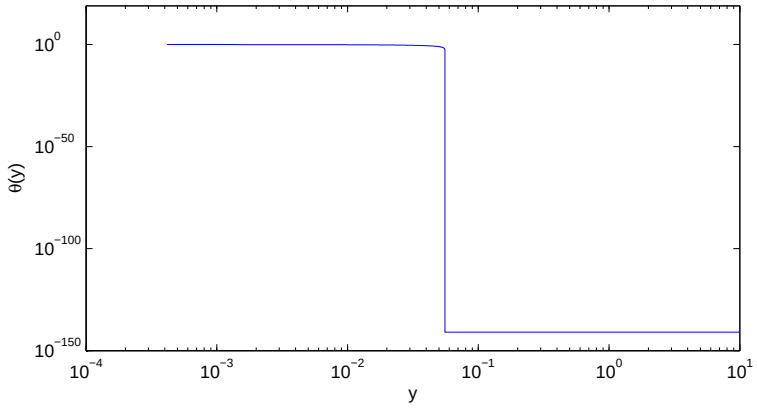

(a) *Numerical solution.*

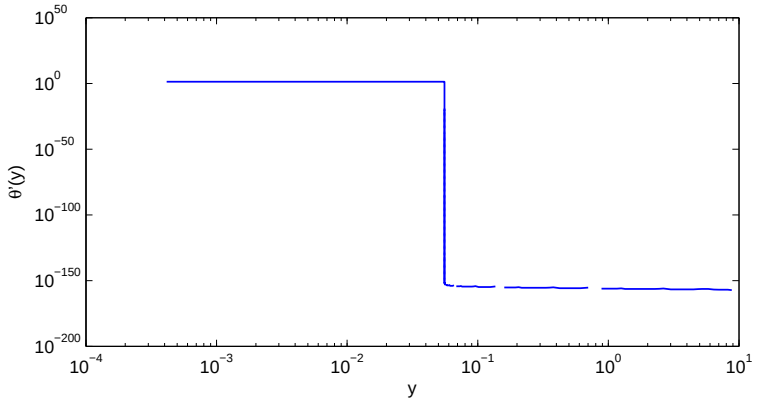

(b) *Numerical approximation of minus the first derivative.*

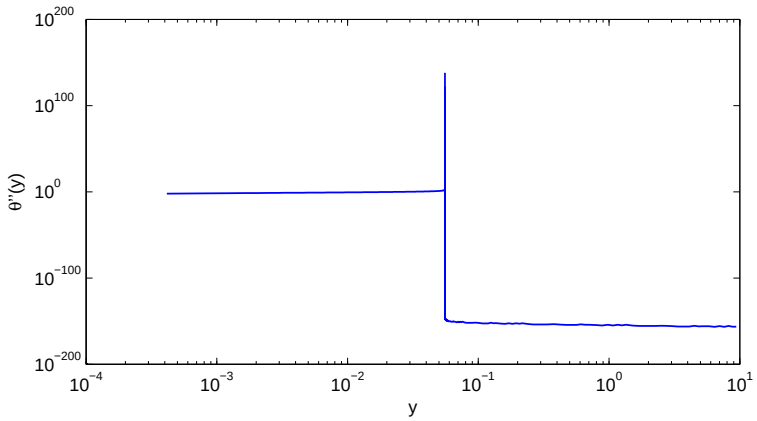

(c) *Numerical approximation of the second derivative.*

Fig. 7. Solution and its derivatives for $\gamma = 18$. Missing points correspond to negative values of $-\theta_y(y)$ and $\theta_{yy}(y)$

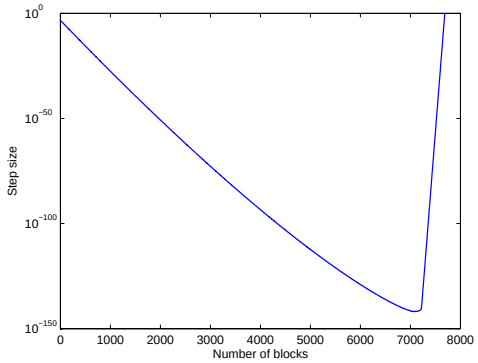

(a) order = 4.

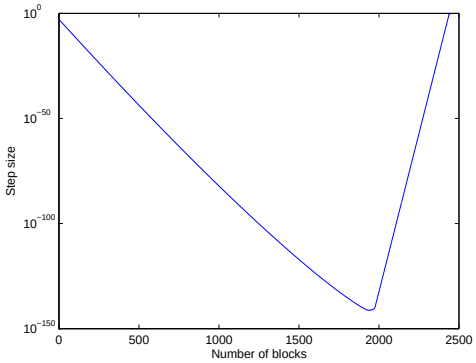

(b) order = 6.

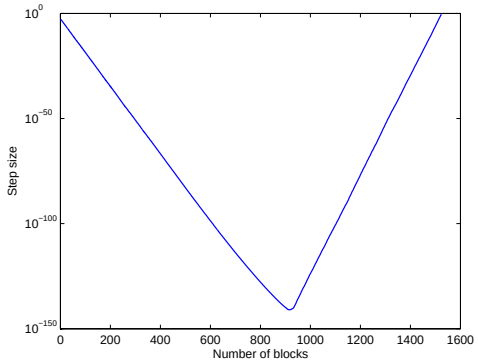

(c) order = 8.

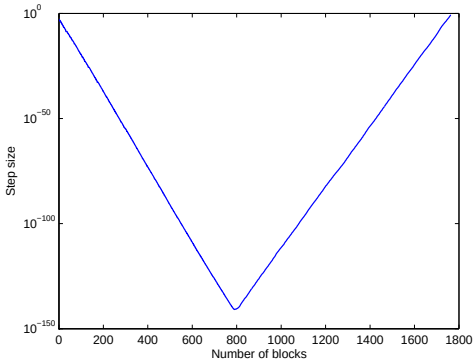

(d) order = 10.

Fig. 8. Step size variation for each block, $\gamma = 18$.